

Modified spontaneous emission in erbium-doped SiO₂ spherical colloids

M. J. A. de Dood,^{a)} L. H. Slooff,^{b)} and A. Polman

FOM Institute for Atomic and Molecular Physics, Kruislaan 407, 1098 SJ Amsterdam, The Netherlands

A. Moroz^{c)} and A. van Blaaderen

FOM Institute for Atomic and Molecular Physics, Kruislaan 407, 1098 SJ Amsterdam, The Netherlands and Physics and Chemistry of Condensed Matter, Debye Institute, Utrecht University, P.O. Box 80.000, 3508 TA Utrecht, The Netherlands

(Received 23 July 2001; accepted for publication 25 September 2001)

Spherical SiO₂ colloids with two different diameters (175 nm, 340 nm) were doped with erbium at different concentrations. The spheres show sharply peaked photoluminescence centered at 1.535 μm , due to intra-4*f* transitions in Er³⁺. From measurements of the Er decay rate for different Er concentrations the decay rate of isolated Er ions (i.e., in absence of concentration quenching) was determined for the two colloid diameters. The data were compared to spontaneous emission rates derived from calculations of the local optical density of states in the colloids. The calculation predicts a large difference in the spontaneous emission rate for both colloid sizes (61 vs 40 s⁻¹), in perfect agreement with the measured data. © 2001 American Institute of Physics.
[DOI: 10.1063/1.1419033]

Erbium-doped dielectric materials find many applications in optical components, due to their sharp optical emission at 1.5 μm , the standard wavelength in optical telecommunications technology. Recently, Er-doped colloids¹ and microspheres² are being investigated. Small (~ 100 nm diameter) colloids can find applications in nanocomposit materials that can be used to fabricate a polymer optical amplifier,³ while larger colloids or microspheres (>10 μm) can be used to fabricate whispering gallery mode lasers operating at 1.5 μm . Optically active colloids can also find applications as probes in photonic crystals, in which they can be used to probe the (local) optical density of states.

Two important parameters determine the gain performance of Er-doped colloids: the stimulated emission cross section and the emission quantum efficiency. The Er³⁺ intra-4*f* transitions at 1.53 μm are in principle forbidden by the parity selection rule, but mixing with other-parity states makes them slightly allowed. Hence, the transitions have a relatively small optical cross section, and consequently, the excited state of Er³⁺ has a long luminescence lifetime.

For a given material, a measurement of the luminescence lifetime can be made relatively easily, thus providing a quick identification of the emission cross section. However, in practice the lifetime is not only determined by radiative emission, but also by nonradiative processes such as multiphonon relaxation, coupling to defects, or interactions between Er ions,^{4,5} that can all quench the excited state. Furthermore, the radiative emission rate is not a fixed property for a given material, but depends on the optical surrounding of the Er ions. For example, the presence of dielectric boundaries changes the local electric field fluctuations and modifies the spontaneous emission rate.⁶ Changes in decay rate can be determined by calculating the local optical density of states

(LDOS) and then applying Fermi's Golden Rule. The radiative decay rate can then be written in terms of a LDOS $\rho(\omega, r)$ as:

$$W_{\text{rad}}(\mathbf{r}) = \frac{\pi\omega}{\hbar\varepsilon(\mathbf{r})} |D|^2 \rho(\omega, \mathbf{r}) \quad (1)$$

where $\varepsilon(\mathbf{r})$ is the position-dependent dielectric constant, ω is the transition frequency and $|D|^2$ the dipole matrix element of the transition involved. This matrix element is determined by the interaction of Er³⁺ ions with the coordinating matrix, while the macroscopic $\rho(\omega, \mathbf{r})$ and $\varepsilon(\mathbf{r})$ are determined by the optical surroundings.

In this letter, we study the modified spontaneous emission of Er ions implanted into spherical SiO₂ colloids. In such small particles, there is a strong interaction between excited Er ions and the colloid-air interface. Using a combined analysis of concentration quenching phenomena and LDOS effects in colloids with two different diameters, we are able to determine absolute values of the radiative and nonradiative decay rates. We find that the spontaneous emission rate for the two sizes differs by 50% and determine the emission cross section.

SiO₂ colloids with a diameter of either 175 or 340 nm ($\pm 5\%$) were made in a reaction between tetraethoxysilane, ammonia, ethanol, and water as described in Ref. 7. The spheres were deposited on Si(100) substrates that were cleaned for 15 min in a 1.0 M KOH solution in ethanol. A droplet of the spheres dissolved in ethanol was put on the substrate and the ethanol was let to evaporate. The 175-nm-SiO₂ colloids were implanted at room temperature with 70 keV Er⁺ ions to fluences of 3.4×10^{14} or 9.1×10^{14} ions/cm². The ion range of 70 keV Er in silica is $r = 48$ nm, and the straggle $\sigma = 11$ nm. The Er peak concentration is 0.2 or 0.5 at. % for the two fluences, respectively. The 340 nm colloids were implanted with 350 keV Er⁺ ions ($r = 160$ nm, $\sigma = 34$ nm) at fluences of 9.0×10^{14} , 2.5×10^{15} , or 4.0×10^{15} ions/cm² (peak concentrations 0.2, 0.5,

^{a)}Electronic mail: dood@amolf.nl

^{b)}Present address: Energy Research Center, Petten, The Netherlands.

^{c)}On leave of absence from: Institute of Physics, Praha, Czech Republic.

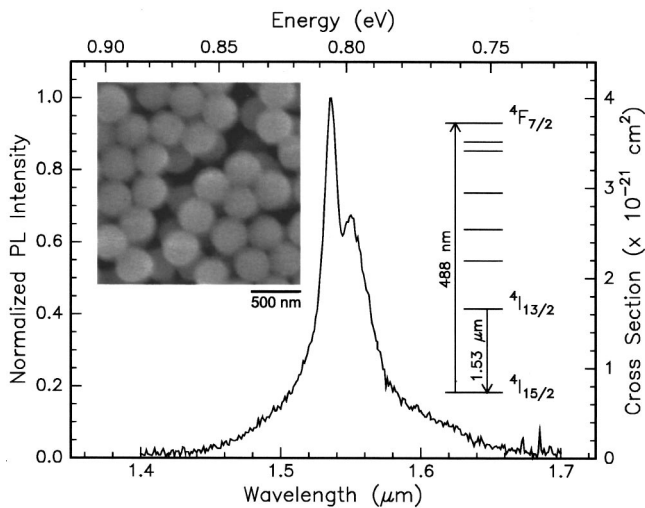


FIG. 1. PL spectrum of Er-implanted SiO₂ colloids (340 nm diameter, 0.2 at. % Er), measured at room temperature under 488 nm excitation. The inset shows a SEM image of 340-nm-diameter colloids.

or 0.8 at. %). After implantation the samples were annealed in a vacuum furnace (pressure $< 5 \times 10^{-7}$ mbar) at 100 °C for 1 h and at 900 °C for another hour. The inset in Fig. 1 shows a scanning electron microscopy (SEM) image of the 340-nm-diameter colloids.

Photoluminescence (PL) measurements were performed using excitation with the 488 nm line of an Ar ion laser. The pump beam was modulated at 13 Hz using an acousto-optic modulator. The PL signal was focused onto the entrance slit of a 48-cm-grating monochromator and detected with a liquid-nitrogen cooled Ge detector employing standard lock-in techniques. The spectral resolution of the system was 6 nm. PL decay traces of the luminescence were recorded at the peak of the Er luminescence at 1.535 μm and averaged using a digitizing oscilloscope. The overall time response of the system was measured to be 30 μs. All decay traces showed single-exponential behavior.

Figure 1 shows a PL spectrum of 340 nm colloids implanted to a peak concentration of 0.2 at. % Er. The Er ions are excited into the $^4F_{7/2}$ level as shown in the inset. The emission is due to transitions from the first excited state ($^4I_{13/2}$) to the ground state ($^4I_{15/2}$), peaking at a wavelength of 1.535 μm. Figure 2 shows PL decay rates measured as a function of Er peak concentration for both the 175 nm colloids (open circles) and the 340 nm colloids (closed circles). For both diameters the PL decay rate increases with Er concentration, an effect that is generally known as concentration quenching.^{5,8} It is due to an increased coupling to quenching sites as a result of excitation migration at high Er concentration (see inset in Fig. 2). For example, in silica glasses it is well known that small quantities of OH impurities can act as a quencher for excited Er. This is due to the fact that the first overtone of the O–H stretch vibration is resonant with the $^4I_{13/2} \rightarrow ^4I_{15/2}$ transition in Er³⁺. For low quencher concentration, the decay rate can be written as:

$$W_{\text{tot}} = W_r + W_i + 8\pi C_{\text{Er-Er}}[\text{Er}][Q], \quad (2)$$

with W_r the radiative rate, W_i the internal nonradiative rate, e.g., due to multiphonon relaxation or coupling to defects, $C_{\text{Er-Er}}$ a coupling constant, and $[\text{Er}]$ and $[Q]$ the Er and

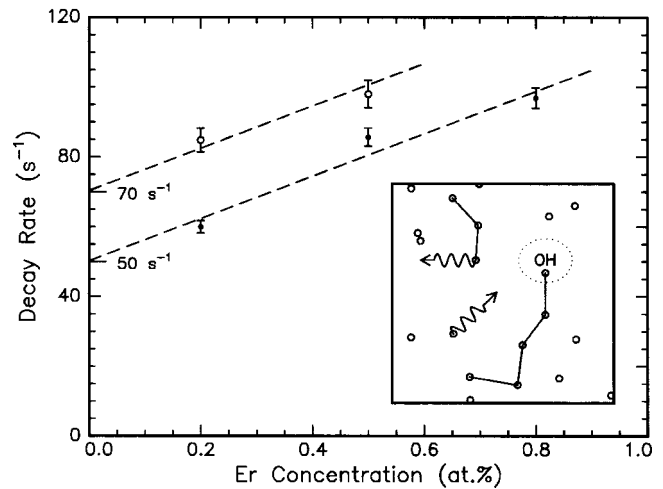


FIG. 2. PL decay rates measured at 1.535 μm for Er implanted colloids as function of Er peak concentration. Data are shown for 175 nm colloids (open circles) and 340 nm colloids (closed circles). The dashed lines are fits to the data according to Eq. (1) assuming an identical slope for both data sets, but different vertical offsets. The inset shows a schematic of the concentration quenching process: excitation migration among Er ions followed by quenching at an OH impurity.

quencher concentration, respectively. The dashed lines in Fig. 2 are fits using Eq. (2), assuming the same slope but a different offset for each type of sample. The fact that both data sets can be described by the same slope indicates that the quencher concentration in 175 and 340 nm colloids is the same, which is expected, as the fabrication procedure for the two sizes is similar. Using a typical value for $C_{\text{Er-Er}}$ from the literature ($10^{-39} \text{ cm}^6 \text{ s}^{-1}$)⁹ we find a quencher concentration of 100 ppm. Assuming the dominant quencher is OH this is a reasonable value, as the colloids were prepared in a wet-chemical reaction.

The vertical intercepts of the fits in Fig. 2 represent the Er decay rates in the absence of concentration quenching ($W_r + W_i$): they are 70.4 s⁻¹ (14.2 ms) and 50.3 s⁻¹ (19.9 ms) for 175 and 340 nm colloids, respectively, and are listed in Table I under $W_{\text{tot}}^{\text{Er}=0}$. These rates can now be compared to calculated values of W_r that can be derived as described below.

Figure 3 shows a calculation of the LDOS in spherical silica colloids, calculated using a Green's function approach.¹⁰ The factor $\epsilon(\mathbf{r})$ is included in the definition of the LDOS [see Eq. (1)], making the LDOS directly proportional to the radiative decay rate. Since the polarization of the emitted radiation is randomly oriented, due to the amorphous structure of the silica glass network, integration over both polarizations is done.

In Fig. 3, the LDOS is plotted for a vacuum wavelength of $\lambda_0 = 1.535 \mu\text{m}$ as a function of radial distance for the two different colloid diameters. The colloids (refractive index n

TABLE I. Measured and calculated Er luminescence decay rates for two different colloid diameters (175 nm, 340 nm).

Colloid diameter (nm)	$f_{1.45}^i$	$W_{\text{tot}}^{\text{Er}=0}$ (s ⁻¹)	W_r (s ⁻¹)	$W_i^{\text{Er}=0}$ (s ⁻¹)
175	1.13	70	61	9
340	0.74	50	40	10

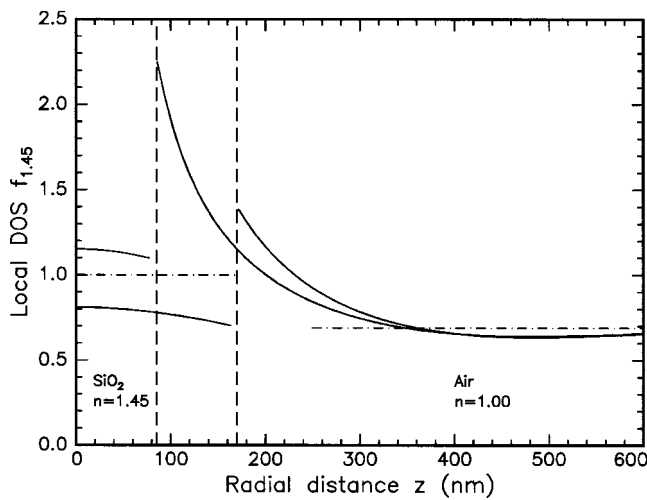


FIG. 3. Polarization-averaged local optical density of states as function of radial position for SiO_2 colloids ($n=1.45$) in air ($n=1.00$), calculated at a vacuum wavelength of $1.535 \mu\text{m}$. Data are shown for colloid diameters of 175 and 340 nm.

$=1.45$) are surrounded by air ($n=1.00$), and the LDOS is normalized to the LDOS in bulk silica (defined as $f_{1,45}=1$). As can be seen, the value of the LDOS inside the colloid differs strongly between spheres of different size. Depending on the size, the LDOS is smaller or larger than the LDOS for bulk SiO_2 . For a given size, not much variation in the LDOS is observed inside the sphere. This can be explained by the fact that for both colloid sizes $2\pi r \leq \lambda_0/n$ (with r the colloid radius), hence no Mie resonances are observed. Assuming that the Er ions are distributed homogeneously over the SiO_2 sphere, the effect of the sphere on the radiative rate can be calculated by integrating the LDOS in Fig. 3 over the sphere volume. For a 175 nm sphere the calculation yields $f_{1,45}^i = 1.13$, while for a 340 nm sphere a value of $f_{1,45}^i = 0.74$ is found. These data are also listed in Table I.

Using these two LDOS factors, the radiative rates in the colloids can be calculated, using as input the radiative rate of Er in bulk SiO_2 ($54 \pm 10 \text{ s}^{-1}$) that we have previously determined.¹¹ An identical rate ($55 \pm 5 \text{ s}^{-1}$) was derived from our analysis of data by Vredenberg *et al.*,¹² described in Ref. 11. From the fact that the PL spectrum for the colloids in Fig. 1 is identical to that of the Er-implanted SiO_2 in our previous work¹¹ we conclude that the local environment in both materials is similar, and that therefore the bulk decay rate of 54 s^{-1} can also be applied to the silica glass used for the colloids. Multiplying this decay rate with the LDOS factors of 1.13 and 0.74 found above gives the purely radiative decay rate in the two types of colloids: $W_r = 61 \text{ s}^{-1}$ (175 nm spheres) and $W_r = 40 \text{ s}^{-1}$ (340 nm spheres). These data are summarized in Table I. Using the radiative rate for Er in bulk SiO_2 and the Fuchtbauer–Ladenberg equation¹³ we can derive a peak cross section of $4.0 \times 10^{-21} \text{ cm}^2$. This value was used to provide a cross-section scale in Fig. 1.

Several conclusions can be drawn by comparing these numbers with the data in Fig. 2. First, the vertical separation between the two linear curves through the data for the two types of colloids is equal to $20 \pm 5 \text{ s}^{-1}$, which is identical to the difference between the radiative rates calculated above

(21 s^{-1}). This provides clear evidence that the data can be consistently described by the LDOS model. Second, subtracting for the two colloid diameters the measured decay rate in absence of concentration quenching ($W_{\text{tot}}^{\text{Er}=0}$) from the calculated radiative rate (W_r) (see Table I), we find the intrinsic nonradiative decay rate W_i ; it amounts to 9 or 10 s^{-1} for the 175 and 340 nm colloids, respectively (see Table I). The relative error on these values is $\pm 5 \text{ s}^{-1}$, the absolute error $\pm 10 \text{ s}^{-1}$. These values for W_i are consistent with the fact that identical intrinsic nonradiative decay rates are expected for both colloid diameters as they are fabricated in an identical way. This again shows that the data in Fig. 2 can be consistently described by the LDOS model.

Finally, we determine the luminescence quantum efficiency (QE) of excited Er. Although the QE has a relatively large error bar ($\pm 10\%–20\%$) due to the uncertainty in W_i , it can be concluded that (1) in absence of concentration quenching the QE is on the order of 80%, (2) the 175 nm colloids have larger QE than the 340 nm colloids, and (3) increasing the concentration from zero to, e.g., 0.5 at. % reduces the quantum QE by some 20%.

In conclusion, we have doped silica colloids with optically active Er ions emitting at $1.535 \mu\text{m}$. Photoluminescence decay measurements as a function of Er concentration are consistent with a concentration quenching model that simultaneously fits the data for both colloid sizes. From the data, the Er decay rate in the absence of concentration quenching was determined. This decay rate was compared with the radiative decay rate derived from calculations of the LDOS in the colloids. The LDOS calculation predicts a large difference in the radiative decay rate for both sizes (61 vs 40 s^{-1}), in perfect agreement with the measured data. This letter shows that by careful consideration of changes in the LDOS it is possible to achieve an accurate quantitative determination of radiative and nonradiative decay processes of Er in silica glass.

This work is part of the research program of FOM and has been financially supported by NWO and the ESPRIT Program of the European Union.

¹L. H. Slooff, M. J. A. de Dood, A. van Blaaderen, and A. Polman, *Appl. Phys. Lett.* **76**, 3682 (2000).

²M. Cai, O. Painter, and K. H. Vahala, *Phys. Rev. Lett.* **85**, 74 (2000).

³L. H. Slooff, Ph.D. thesis, Utrecht University, 2000.

⁴J. C. Wright, in *Radiationless Processes in Molecules and Condensed Phases*, edited by F. K. Fong (Springer, Heidelberg, 1976), p. 239.

⁵H. C. Chow and R. C. Powell, *Phys. Rev. B* **21**, 3785 (1980).

⁶For a review see, W. L. Barnes, *J. Mod. Opt.* **4**, 661 (1998); for the specific case of Er see: E. Snoeks, A. Lagendijk, and A. Polman, *Phys. Rev. Lett.* **74**, 2459 (1995).

⁷A. van Blaaderen and A. Vrij, *Langmuir* **8**, 2921 (1993).

⁸E. Snoeks, P. G. Kik, and A. Polman, *Opt. Mater.* **5**, 159 (1996).

⁹V. P. Gapontsev, A. A. Izyneev, Yu. E. Sverchov, and M. R. Syrtlanov, *Sov. J. Quantum Electron.* **11**, 1101 (1981).

¹⁰A. Moroz, *Europhys. Lett.* **46**, 419 (1999).

¹¹M. J. A. de Dood, L. H. Slooff, A. Moroz, A. van Blaaderen, and A. Polman, *Phys. Rev. A* **64**, 033807 (2001).

¹²A. M. Vredenberg, N. E. J. Hunt, E. F. Schubert, D. C. Jacobson, J. M. Poate, and G. J. Zydzik, *Phys. Rev. Lett.* **71**, 517 (1993).

¹³ $W_{\text{rad}} = 8\pi n^2/c^2 \int \nu^2 \sigma(\nu) d\nu$, where n is the host refractive index ($n=1.45$), c is the speed of light, and ν is the optical frequency of the transition involved.